Supplementary Information

Synergistic effect between polyvinyl pyrrolidone and oxygen vacancies on improving oxidase-mimetic activity of flower-like CeO_2 Nanozymes

Mingyun Zhu,[a] Yifeng Wen,[a] Shugui Song,[a] Anqi Zheng,[a] Jingcang Li,[a] Weiwei Sun,[a] Yunqian Dai,[b,*] Kuibo Yin,[a,*] Litao Sun,[a,*]

[a]SEU-FEI Nano-Pico Center, Key Laboratorsy of MEMS of Ministry of Education, Southeast University, Nanjing, 210096, P. R. China

[b]School of Chemistry and Chemical Engineering, Southeast University, Nanjing, 211189, P. R. China

*Address corresponding to: yinkuibo@seu.edu.cn, daiy@seu.edu.cn, and slt@seu.edu.cn

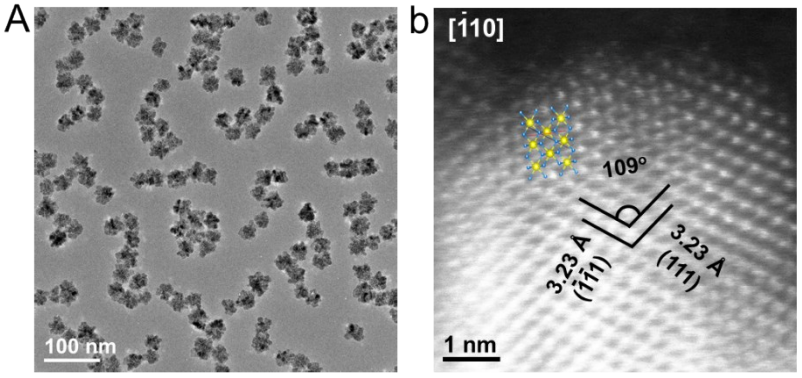

Fig. S1 (a) TEM image, (b) High-resolution STEM image of the one representative CeO_2 nanoflower.

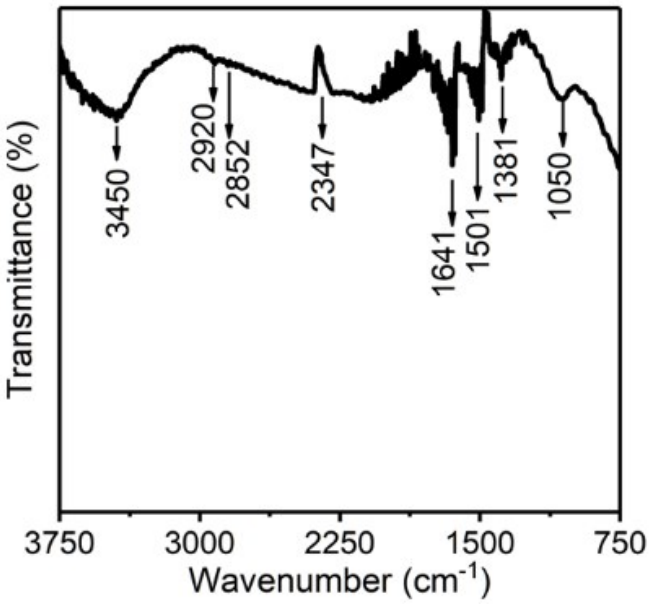

Fig. S2 FTIR spectrum of CeO_2 nanoflowers.

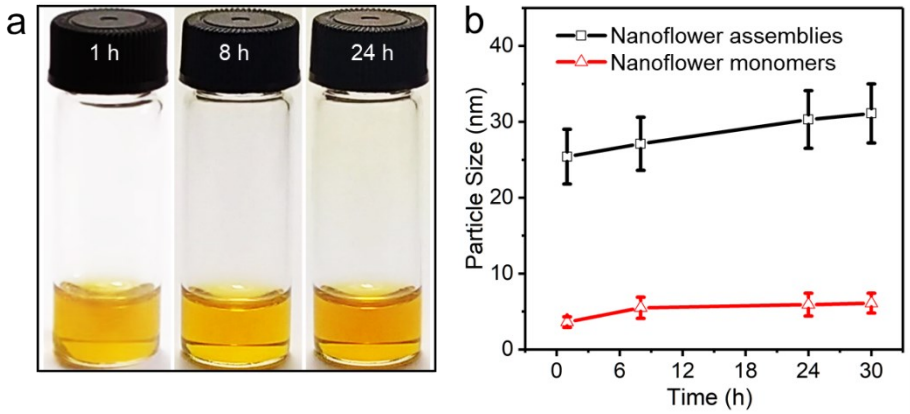

Fig. S3 (a) Optical images and (b) average-size evolutions of nanoflower assemblies and monomers obtained at different solvothermal durations.

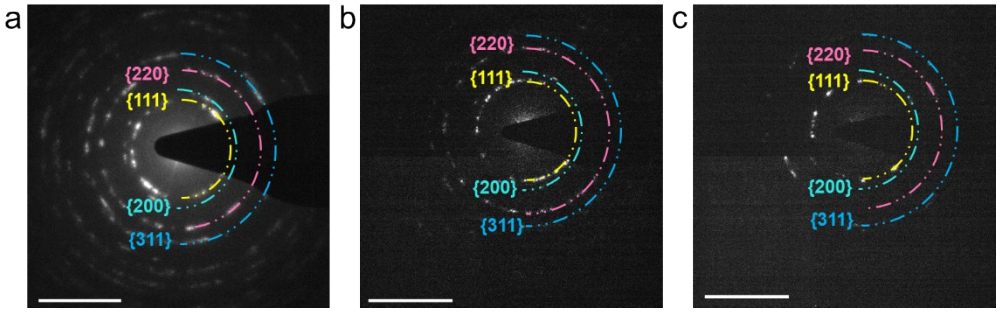

Fig. S4 SAED patterns of CeO_2 nanoflowers obtained at different solvothermal durations: (a) 1 h, (b) 8 h, and (c) 24 h. Scale bar: 5 1/nm.

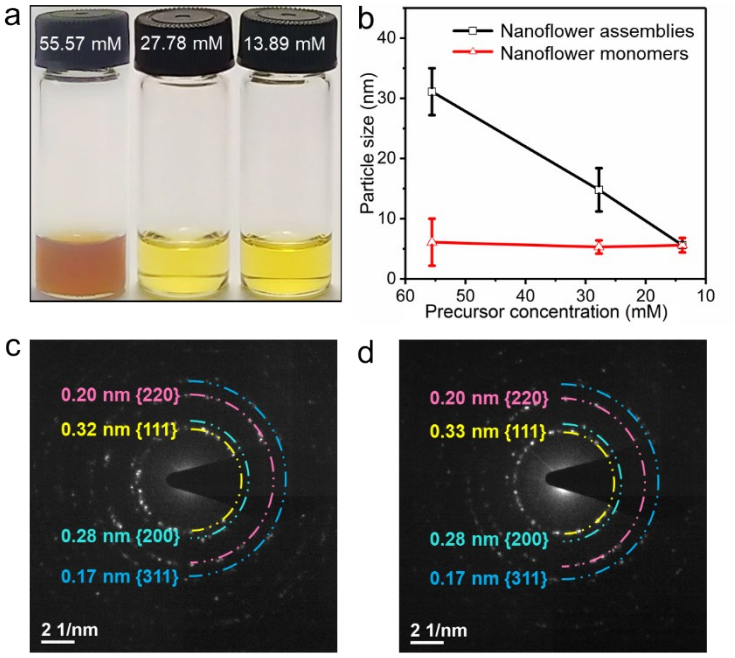

Fig. S5 (a) Optical images, (b) average-size evolutions, and (c-d) SAED patterns of CeO_2 nanoflowers obtained from different precursor concentrations: (c) 27.78 mM, (d) 13.89 mM.

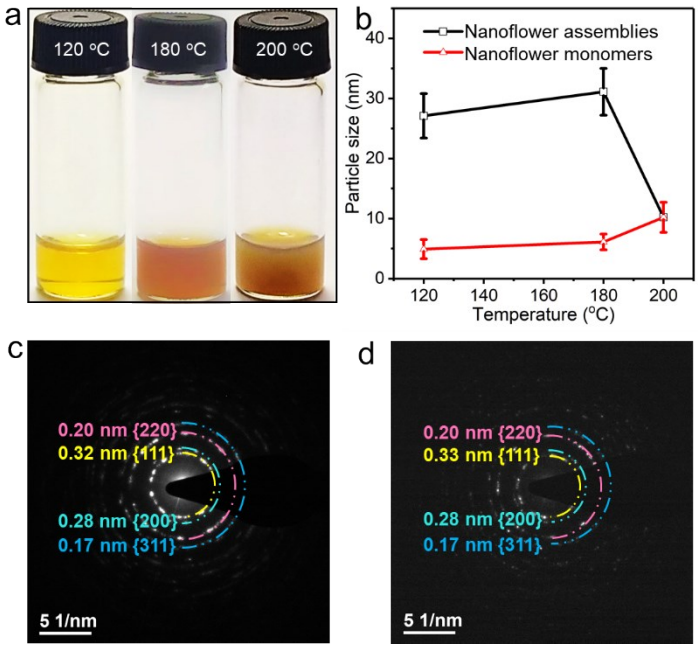

Fig. S6 (a) Optical images, (b) average-size evolutions, and (c–d) SAED patterns of CeO_2 nanoflowers obtained at different reaction temperatures: (c) 120 °C, (d) 200 °C.

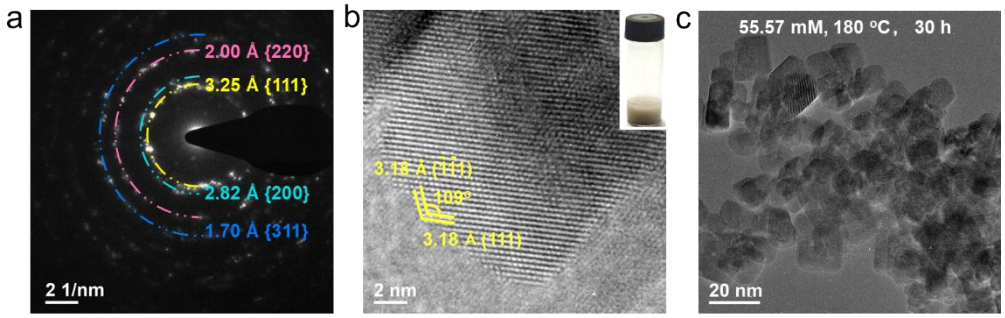

Fig. S7 (a) SAED pattern, and (b–c) HRTEM images of CeO_2 nanocubes obtained in the absence of PVP. Inset in (b) is the corresponding optical image.

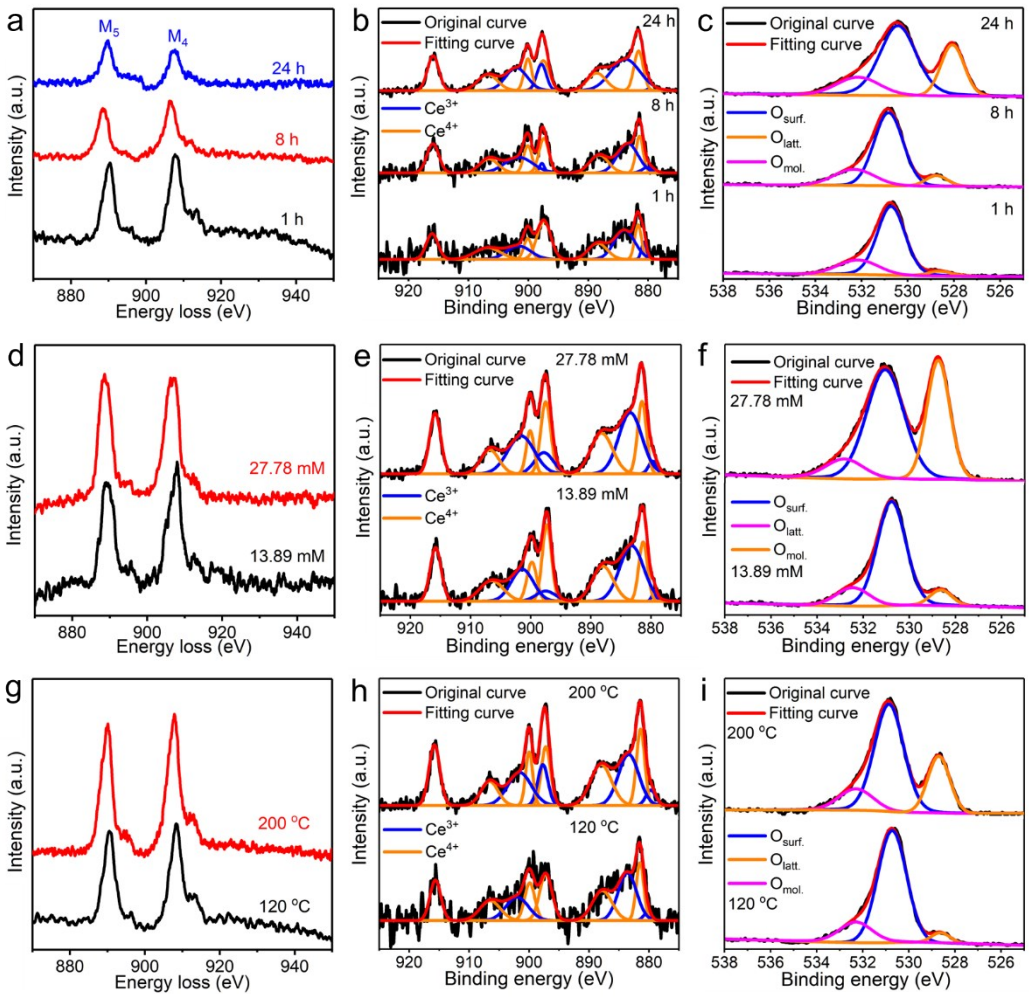

Fig. S8 (a, d and g) EELS, and (b–c, e–f, and h–i) XPS spectra of a CeO_2 nanoflowers obtained at different conditions: (a–c) at different reaction durations, (d–f) from different precursor concentrations, (g–h) at different solvothermal temperatures. Specifically, EELS for Ce-$M_{5,4}$ edge, and XPS for Ce 3*d* and O 1*s*.

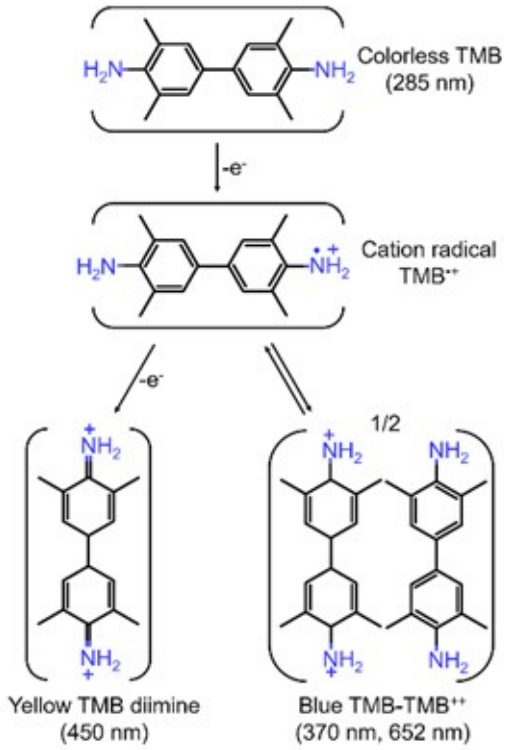

Fig. S9 Oxidation process of TMB.

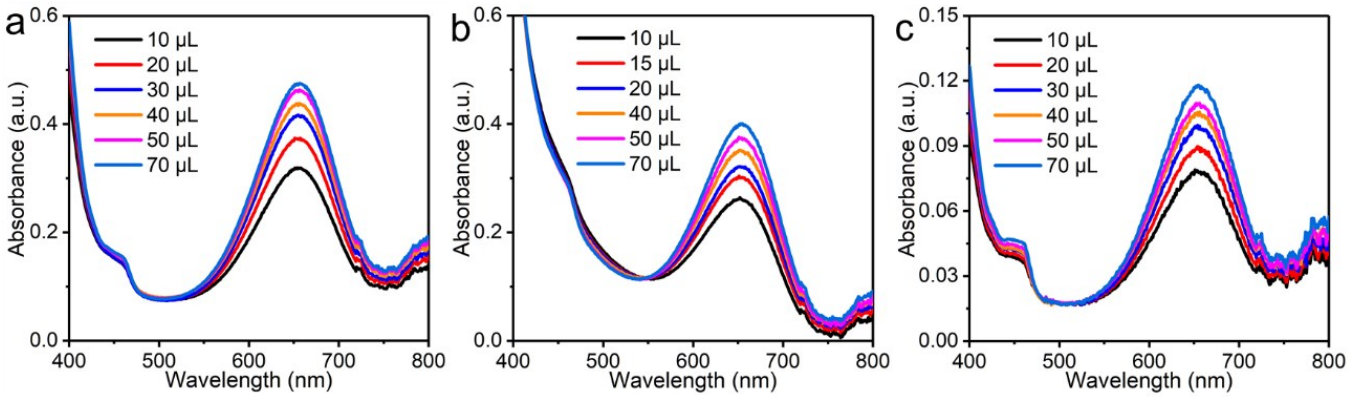

Fig. S10 TMB-dependent UV-vis absorption spectra of the mixture containing (a) 2 μmol of 31.1-nm CeO_2 nanoflowers, (b) 0.5 μmol of 5.6-nm CeO_2 nanocubes, and (c) 2 μmol of 10.1-nm CeO_2 nanocubes. The concentration of the used TMB is 10 mM.

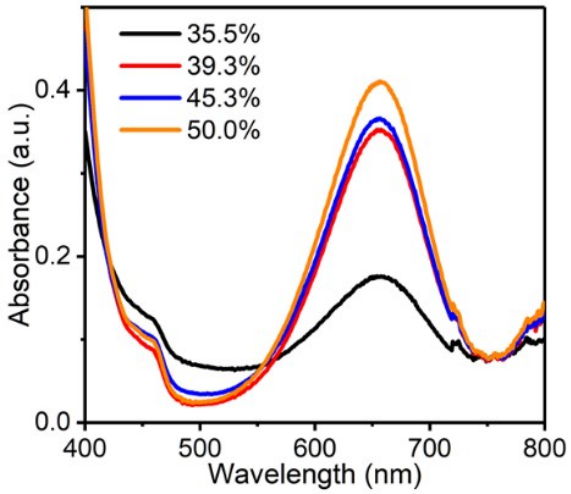

Fig. S11 UV-vis absorption spectra of the TMB solutions catalyzed by CeO_2 nanoflowers with different Ce(Ⅲ) percentages.

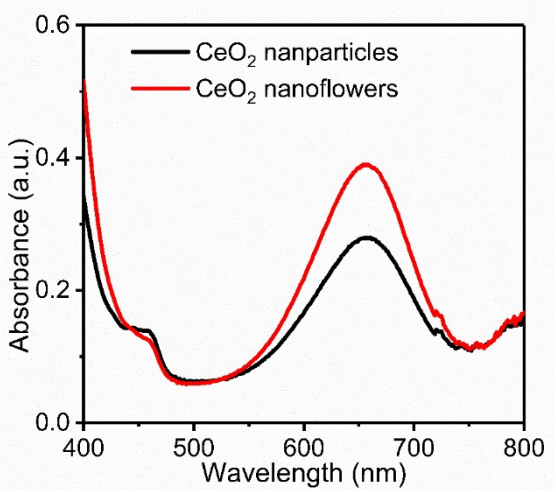

Fig. S12 UV-vis spectra of TMB solution catalyzed by CeO_2 nanoparticles with different structures. Nanoflowers: 39.8% Ce(Ⅲ) and 0.93 for M_5/M_4, nanoparticles: 39.9% Ce(Ⅲ) and 0.93 for M_5/M_4.

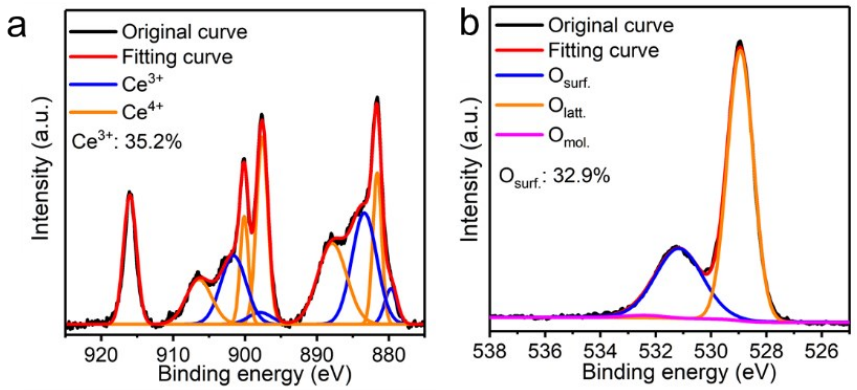

Fig. S13 XPS spectra for (a) Ce 3*d* and (b) O 1*s* of the PVP-free CeO_2 nanocubes.

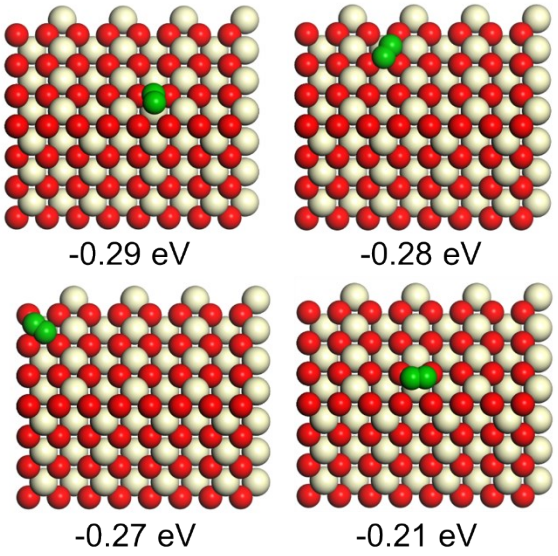

Fig. 14 The adsorption energy of O_2 on the {220} facet in different configuration models. Green: O atoms within O_2, red and light yellow: lattice O and Ce atoms within CeO_2.

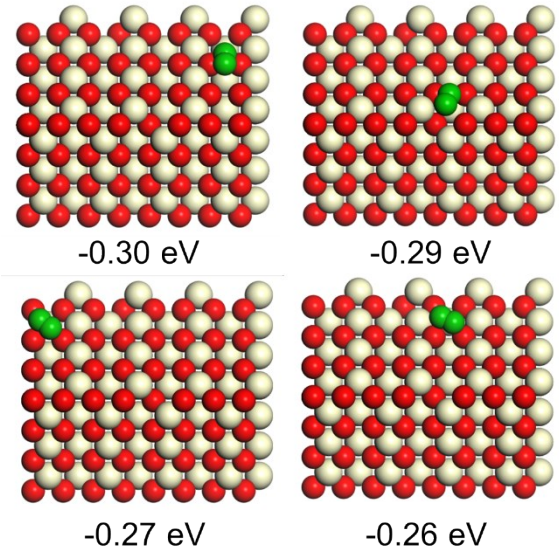

Fig. 15 The adsorption energy of O_2 (green) on the oxygen-deficient {220} facet in different configuration models. Green: O atoms within O_2, red and light yellow: lattice O and Ce atoms within CeO_2.

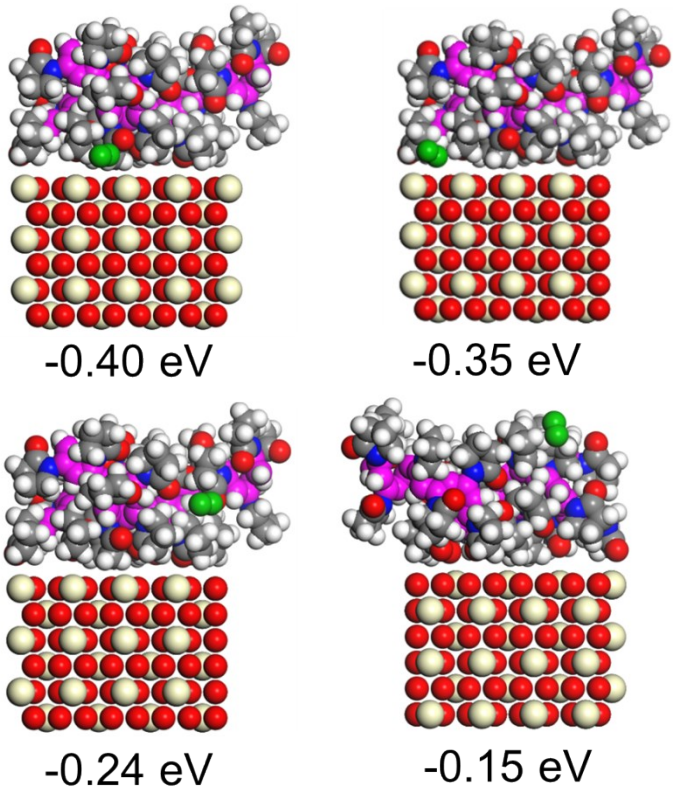

Fig. 16 The adsorption energy of O_2 (green) on the oxygen-deficient {220} facet with the existence of PVP in different configuration models. Green: O atoms within O_2; red: O atoms within CeO_2 and PVP; light yellow: lattice Ce atoms with CeO_2; grey, blue and white: C, N and H atoms within PVP

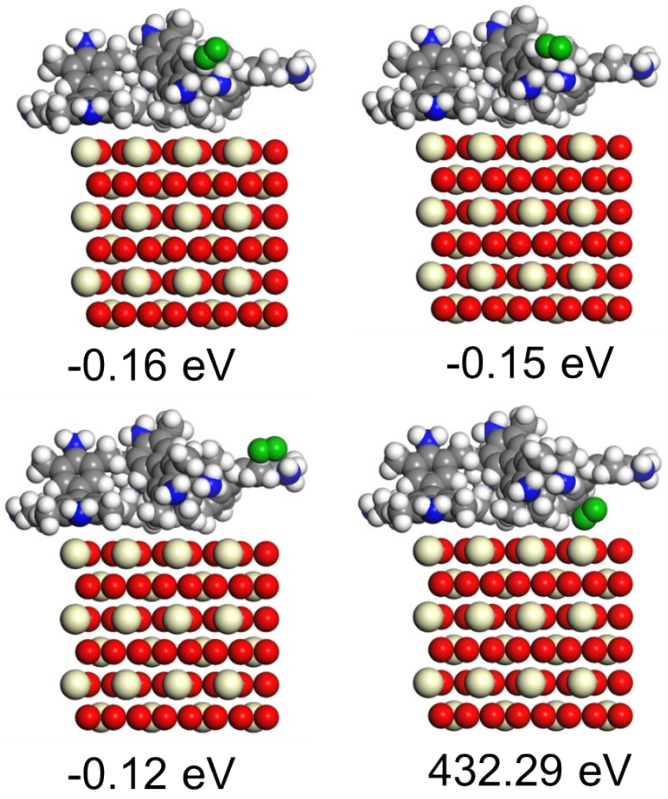

Fig. 17 The adsorption energy of O_2 (green) on the oxygen-deficient {220} facet with the existence of TMB in different configuration models. Green: O atoms within O_2; red and light yellow: lattice O and Ce atoms within CeO_2; grey, blue and white: C, N and H atoms within TMB.